

e-ISSN : 2320-0847

p-ISSN : 2320-0936



# AJER

*American Journal of Engineering Research*

## Volume-2 Issue-1



# AJER

*American Journal of Engineering Research*

American Journal of  
Engineering Research

# Editorial Board

## American Journal of Engineering Research (AJER)

**Dr. Jonathan Okeke  
Chimakonam**

Qualification: PHD  
Affiliation: University of Calabar  
Specialization: Logic, Philosophy of  
Maths and African Science,  
Country: Nigeria

**Dr. ABDUL KAREEM**

Qualification: MBBS, DMRD, FCIP, FAGE  
Affiliation: UNIVERSITI SAINS Malaysia  
Country: Malaysia

**Dr. sukhmander singh**

Qualification: Phd  
Affiliation: Indian Institute Of  
Technology, Delhi  
Specialization : PLASMA PHYSICS  
Country: India

**Dr. Nwachukwu Eugene Nnamdi**

Qualification: Phd  
Affiliation: Michael Okpara University of  
Agriculture, Umudike, Nigeria  
Specialization: Animal Genetics and  
Breeding  
Country: Nigeria

**Dr. June II A. Kiblasan**

Qualification : Phd  
Specialization: Management, applied  
sciences  
Country: PHILIPPINES

**Dr. Narendra Kumar Sharma**

Qualification: PHD  
Affiliation: Defence Institute of Physiology  
and Allied Science, DRDO  
Specialization: Proteomics, Molecular  
biology, hypoxia  
Country: India

**Prof. Dr. Shafique Ahmed Arain**

Qualification: Postdoc fellow, Phd  
Affiliation: Shah Abdul Latif University  
Khairpur (Mirs),  
Specialization: Polymer science  
Country: Pakistan

**Dr. Alcides Chaux**

Qualification: MD  
Affiliation: Norte University, Paraguay,  
South America  
Specialization: Genitourinary Tumors  
Country: Paraguay, South America

**Dr. Md. Nazrul Islam Mondal**

Qualification: Phd  
Affiliation: Rajshahi University, Bangladesh  
Specialization: Health and Epidemiology  
Country: Bangladesh

## CONTENTS

### Volume-2 Issue-1

S.No.	Title Name	Page No.
01.	<b>COMPARATIVEANALYSIS OF ADVANCED CONTROLLERS IN A HEAT EXCHANGER</b> Mr. P.Sivakumar, Dr.D.Prabhakaran, Dr. T .Kannadasan	01-06
02.	<b>EFFECT OF TOOL PIN PROFILES AND HEAT TREATMENT PROCESS IN THE FRICTION STIR WELDING OF AA 6061 ALUMINIUM ALLOY</b> P.Prasanna, Dr.Ch.Penchalayya, Dr.D.Anandamohana Rao	07-15
03.	<b>Comparative Study of The Effects Of Sawdust From Two Species Of Hard Wood And Soft Wood As Seeding Materials On Biogas Production</b> Oluwaleye, Iyiola Olusola, and Awogbemi, Omojola	16-21

## COMPARATIVE ANALYSIS OF ADVANCED CONTROLLERS IN A HEAT EXCHANGER

Mr. P.Sivakumar, Dr.D.Prabhakaran, Dr. T .Kannadasan

*M. Tech Scholar, Department of Chemical Engineering, Coimbatore Institute of Technology.  
Associate Professor, Department of Chemical Engineering, Coimbatore Institute of Technology,  
Professor and Head, Department of Chemical Engineering, Coimbatore Institute of Technology,*

**Abstract:** Temperature control of the shell and tube heat exchanger is characteristics of nonlinear, time varying and time lag. Since the temperature control with conventional PID controller cannot meet a wide range of precision temperature control requirement, we design temperature control system of the shell and tube heat exchanger by combining fuzzy and PID control methods in this paper. The simulation and experiments are carried out; making a comparison with conventional PID control showing that fuzzy PID strategy can efficiently improve the performance of the shell and tube heat exchanger.

**Keywords:** Control algorithm, Fuzzy logic, PID Controller, Tuning

### I. INTRODUCTION

In many industrial process and operations Heat exchanger is one of the simplest and important unit [1] for the transfer of thermal energy. There are different types of heat exchangers used in industries; the shell and tube heat exchanger system being most common. The main purpose of exchanger is to maintain specific temperature conditions, which is achieved by controlling the exit temperature of one of the fluids (mainly hot fluid) in response to variations of the operating conditions.

The temperature control of heat exchanger is nonlinear, time varying and time delay system. For these situations, nonlinear control strategies can provide significant improvements over PID control [2], [12]. Control of temperature using PID controllers, compared to other methods, is more effective and economical.

The heat exchangers need to respond to highly non linear features and work well under different operating points. In order to achieve a wide range of high accurate temperature, we combine neuro-fuzzy control and PID control methods. The main design is to assume neuro-fuzzy reasoning control methods according to different error 'e' and error change 'ec' to get self-tuning PID parameter based on conventional PID controller. The simulation of the controller was accomplished carrying out experiments in an actual heat exchanger system.

### II. TEMPERATURE CONTROL SYSTEM

#### A. Principal of temperature control in shell and tube heat exchanger

The control of temperature in a shell-and-tube heat exchanger is demonstrated in figure 1, with cold water flowing on the tube side and steam on the shell side [5] where steam condenses and heats the water in the tubes. The controlled variable is the tube-side outlet temperature, and the manipulated variable is the steam flow rate on the shell-side.

$$M_c C_p (T_{in} - T_{out}) = M_s A \quad (1)$$

where,  $M_c$ ,  $M_s$ ,  $C_p$ ,  $T_{in}$  and  $T_{out}$  refer to cold water flow rate, steam flow rate, specific heat of water, inlet water temperature, and outlet water temperature respectively.

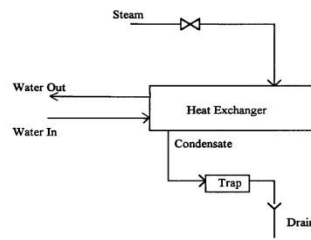


Fig.1.Shell and Tube heat exchanger

The dynamics of the process are complex because of various nonlinearities introduced into the system. The installed valve characteristic of the steam may not be linear [3]. Dead-time depends on the steam and water flow rates, the location and the method of installation of the temperature-measuring devices. To take into account the non-linearity and the dead-time, gain scheduling features and dead-time compensators have to be added. Also, the process is subjected to various external disturbances such as pressure fluctuations in the steam header, disturbances in the water line, and changes in the inlet steam enthalpy and so on.

**B. Mathematical Model of heat exchanger**

The total heat in the heat exchanger system can be expressed as equation 2. [5].

$$Q_f = Q_s + \sum_{i=1}^n C_i \rho_i V_i dT_i \tag{2}$$

where,  $Q_f$ ,  $Q_s$ ,  $C$ ,  $\rho$ ,  $V$  and  $dT$  refer to total system heat productivity, total system heat dissipating capacity, specific heat capacity, heat transfer medium density, volume, and temperature variation.

Total system heat dissipating capacity  $Q_s$  is given by equation 3.

$$Q_s = \sum_{i=1}^n k_i A_i (T_{in} - T_{out}) \tag{3}$$

where,  $k_i$  and  $A_i$  refer to heat transfer coefficient, heat transfer area of the heat exchanger system.

The heat exchanger equations can be expressed as in equation 4. [12]

$$C_w \rho_w q_w (T_{wo} - T_{wi}) d\tau = C_f \rho_f q_f (T_{fo} - T_{fi}) d\tau \tag{4}$$

where, the subscripts  $W$  and  $f$  refer to cold and hot water of the heat exchanger system. Therefore considering all above equations, the differential equation of the shell and tube heat exchanger is shown in equation 5.

$$\frac{dT}{d\tau} + FT = N(x - \tau) \tag{5}$$

where,

$$F = \frac{k_i A_i}{C_o \rho_o V} \tag{6}$$

The transfer function of controlled object can be derived from equation 5, it is described as the first-order with pure time delay, expressed as equation 7.

$$G(s) = \frac{K}{1 + Ts} e^{-\tau s} \tag{7}$$

where,  $T$ ,  $K$  and  $\tau$  refer to time constant, system gain, and delay time.

**III. INTELLIGENT CONTROLLERS**

**A. PID Control of Shell and Tube Heat Exchanger**

PID controller is the most popular controller used because it is easy to operate and very robust. Implementation of the latest PID controller is based on a digital design. These digital PID include many algorithms to improve their performance, such as anti wind-up, auto-tuning, adaptive, fuzzy fine-tuning and Neural Networks with the basic operations remaining the same. The performance specifications such as rise

time, overshoot, settling time and error; steady state can be improved by tuning value of parameters  $K_p$ ,  $K_i$  and  $K_d$  of the PID controller. The output is mathematically represented as equation 8 and 9.

$$y(t) = K_p[e(t) + T_d \frac{de(t)}{dt} + \frac{1}{T} \int_0^t e(t)dt] \quad (8) \quad y(t) = K_p e(t) + K_p T_d \frac{de(t)}{dt} + \frac{K_p}{T} \int_0^t e(t)dt \quad (9)$$

**B. Structure and Parts of Self tuning Fuzzy Controller**

Fuzzy logic controller as shown in Figure 2 consists of main four parts fuzzification, rule base, inference engine and de-fuzzification [6], [8].

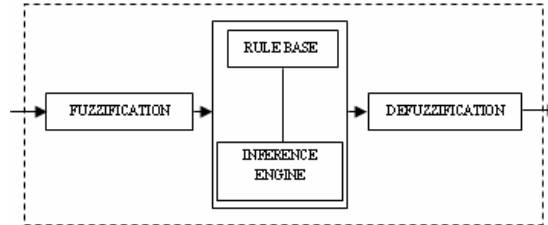


Fig.2.Main Parts of Fuzzy PID Control

Fuzzy PID Self-tuning Control takes error "e" and Change-in-error "ec" as the input of Fuzzy PID controller. Using fuzzy control rules on-line, PID parameters " $K_p$ ", " $K_i$ ", " $K_d$ " are amended, which constitute a self-tuning fuzzy PID controller, the principle of which is shown in Figure 3. The language variable values of error "e" and the error rate of change "ec" is (NB, NM, NS, ZO, PS, PM, PB) seven fuzzy values. And then setting up the suitable fuzzy control table for  $K_p$ ,  $K_i$ ,  $K_d$  three parameters tuning separately[8], [9].According to the fuzzy rules table, appropriate vague and ambiguous methods is to be selected to make dynamic tuning for  $K_p$ ,  $K_i$ ,  $K_d$ .

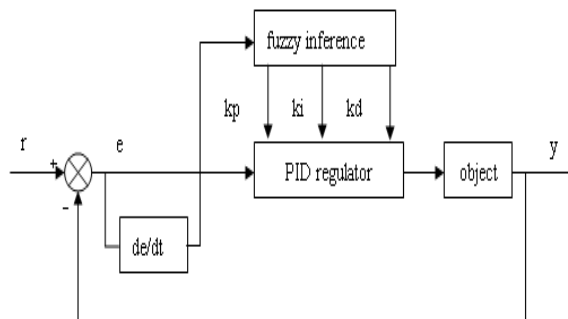


Fig.3.Structure of Fuzzy PID Control

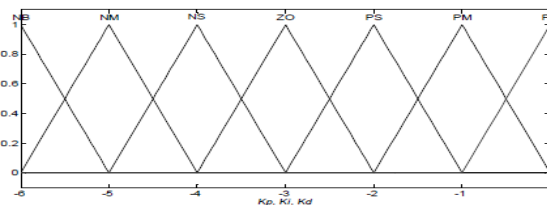


Fig.4.Input membership function for e and ec

The fuzzy controller takes two inputs (e, and error change ec) and three outputs ( $K_p$ ,  $K_i$ ,  $K_d$ ). When the error is large, it is controlled according to the characteristics of PID control where the output value automatically closes to the given value. When the error becomes smaller to a certain extent, the fuzzy control takes effect. The input error, error change and output membership functions use triangular functions, which are shown in figure 4 and 5.

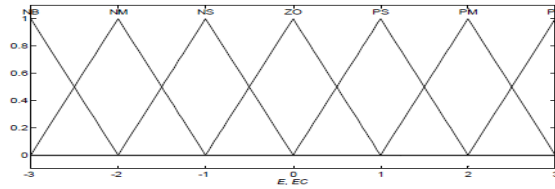


Fig.5.Output membership function for  $K_p, K_i, K_d$

Larger  $K_p$  is chosen to speed up the system response speed. At the same time, in order to avoid the probable differential super-saturation, smaller  $K_i$  is chosen. In order to avoid large overshoot, the integral is limited by setting  $K_d$  is zero.

TABLE 1 THE FUZZY CONTROL RULE FOR  $K_p$

$\Delta x_i$ \ e	ec	NB	NM	NS	ZO	PS	PM	PB
NB		PB	PB	PM	PM	PS	ZO	ZO
NM		PB	PB	PM	PS	PS	ZO	NS
NS		PM	PM	PM	PS	ZO	NS	NS
ZO		PM	PM	PS	ZO	NS	NM	NM
PS		PS	PS	ZO	NS	NS	NM	NM
PM		PS	ZO	NS	NM	NM	NM	NB
PB		ZO	ZO	NM	NM	NM	NB	NB

In order to make the overshoot of the system respond relatively small and to ensure the system response speed,  $K_p$  is set smaller, and  $K_i$  and  $K_d$  values are chosen respectively.

TABLE 2 THE FUZZY CONTROL RULE FOR  $K_i$

$\Delta x_i$ \ e	ec	NB	NM	NS	ZO	PS	PM	PB
NB		NB	NB	NM	NM	NS	ZO	ZO
NM		NB	NB	NM	NS	NS	ZO	ZO
NS		NB	NM	NS	NS	ZO	PS	PS
ZO		NM	NM	NS	ZO	PS	PM	PM
PS		NM	NS	ZO	PS	PS	PM	PB
PM		ZO	ZO	PS	PS	PM	PB	PB
PB		ZO	ZO	PS	PM	PM	PB	PB

In order to make the system have better steady state,  $K_p$  and  $K_i$  are set larger, and to avoid oscillations near the set point,  $K_d$  is set properly. When  $ec$  is small,  $K_d$  is set middle, and when  $ec$  is large,  $K_d$  is set small. According to the given rules, the control rule table of PID parameters can be obtained and the control rules for  $K_p, K_d$  and  $K_i$  is listed in table 1, 2 and 3.

TABLE 3 THE FUZZY CONTROL RULE FOR  $K_d$

$\Delta x_i$ \ e	ec	NB	NM	NS	ZO	PS	PM	PB
NB		PS	NS	NB	NB	NB	NM	PS
NM		PS	NS	NB	NM	NM	NS	ZO
NS		ZO	NS	NM	NM	NS	NS	ZO
ZO		ZO	NS	NS	NS	NS	NS	ZO
PS		ZO						
PM		PB	NS	PS	PS	PS	PS	PB
PB		PB	PM	PM	PM	PS	PS	PB

**Defuzzification**

In this paper, we use the weighted average method to the fuzzy evaluation to get the precise control value with formula as shown in equation 10.

$$u_0 = \frac{\sum_{i=1}^n \mu(u_i) \cdot u_i}{\sum_{i=1}^n \mu(u_i)} \tag{10}$$

Where  $u_i$  is the fuzzy set values,  $\mu(u_i)$  is membership degree of fuzzy values and  $u_0$  is evaluation result. After the three parameters are adjusted by the fuzzy controller, the output control parameters are calculated from the equation 9.

### C. Neuro- Fuzzy Controller

In the field of artificial intelligence, neuro-fuzzy refers to combinations of artificial neural networks and fuzzy logic. Neuro-fuzzy hybridization results in a hybrid intelligent system by combining the human-like reasoning style of fuzzy systems with the learning and connection structure of neural networks. The drawbacks are the complexity and the darkness of their structures. Industries use the PID technique since it is a crisp control. The self tuning of the P, I, D parameters are quite difficult and the resultant control is with overshoot and with large time constants. To avoid we use the combination of Neuro-Fuzzy PID controllers for controlling the temperature in the process.

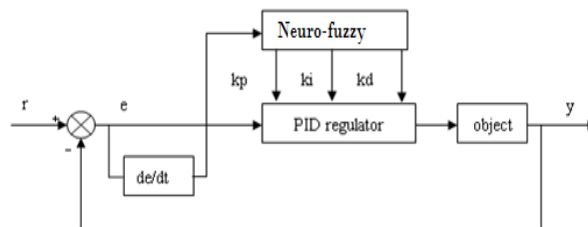


Fig.6. Structure of Neuro-Fuzzy PID Control

## IV. EXPERIMENTAL RESULTS AND DISCUSSIONS

### A. Step Response for the Intelligent Controllers

Comparison between conventional PID, fuzzy PID and Neuro-Fuzzy PID controller's temperature control was performed. According to the analysis fuzzy controller is designed in MATLAB and the fuzzy self-tuning PID control system model is designed by SIMULINK. The step response of the Fuzzy control and conventional control is shown in Figure 7, 8.

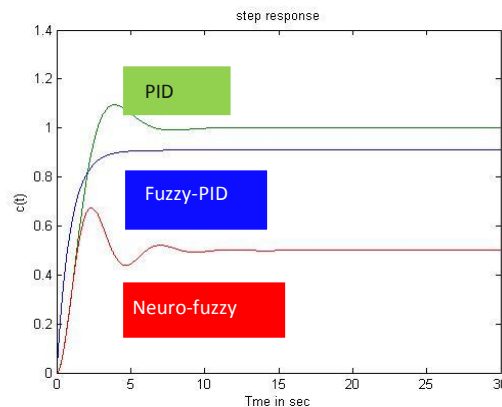


Fig.7. Step Response for the Intelligent Controllers

The initial tuning of the PID controller is accomplished based on the Ziegler-Nicholes method, and the gain coefficients are  $K_p=1.1$ ,  $K_i=0.003$  and  $K_d=52$ . Fuzzy PID Controller has a small overshoot, fast response and the steady state error is less than 1%.

### B. Response of the Temperature control system

The temperature control experiment is conducted in the actual Shell and tube heat exchanger system. The target outlet temperature of heat exchanger is  $60^\circ\text{C}$  and figure 7 shows the response of heat exchanger.

The results suggest that neither the settling time nor control accuracy is satisfied enough when conventional PID controller is used in shell and tube heat exchanger. The steady state error of the PID controller is greater than fuzzy PID. The experimental results shows that fuzzy self-tuning PID control has better dynamic response and steady state error characteristics.

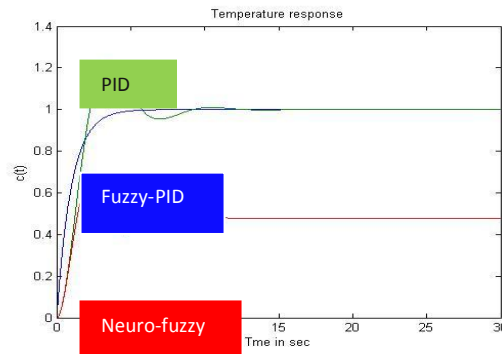


Fig.8.Response of Temperature control

### C. Comparison of various parameters

Table 4 shows the comparison of various parameters from the above graph for the various types of Controllers.

TABLE 4 COMPARISON OF PARAMETERS

Parameters	PID	Fuzzy PID	Neuro Fuzzy PID
Rise Time	1.8	2.6	3.2
Peak over shoot	0.68	0.82	1.2
Settling Time	14	5.8	8.6
Peak Time	2.6	4.1	4.2

### V. CONCLUSION

In this paper we have discussed the design of a temperature control of a shell and tube heat exchanger based on Neuro-fuzzy PID control by comparing it with PID and Fuzzy PID. The analysis fuzzy controller is designed in MATLAB and the fuzzy self-tuning PID control system model is designed by SIMULINK. The results suggested that self-tuning parameter fuzzy PID controller has a smaller system overshoot, faster response and less steady state error thereby making it stronger than conventional PID controller. It was thus concluded that fuzzy self-tuning PID control has better dynamic response and steady state error characteristics. The control rule table of PID parameters was obtained and the control rules for  $K_p$ ,  $K_d$  and  $K_i$  was tabulated. The actual system used obtains a good control effect and can satisfy the requirements of the temperature control system of the shell and tube heat exchanger. support throughout the preparation of this work.

I would like to express my gratitude to Dr.D.Prabhakaran, Associate Professor, Coimbatore Institute of Technology for his motivation and guidance throughout my work.

### REFERENCES

- [1] H. Thal-Larsen, Dynamics of heat exchangers and their models, ASME J. Basic Eng. 1960, pp. 489 – 504.
- [2] M.Chidambaram, and Y.S.N. Malleswara rao, Nonlinear Controllers for heat exchangers, J. Proc. Cont., 1992 vol 2(1), pp 17-21.
- [3] A.W.Alsop, and T.F.Edgar, Non-linear heat exchanger control through the use of partially linearised control variables, Chem. Eng. Commn., vol.75, 1998, pp 155 – 170.
- [4] Wang Li-Xin, Adaptive fuzzy systems and control: Design and stability analysis [M], Prentice-Hall Englewood cliffs NewJersey 1994.
- [5] H. Yamashita, R. Izumi, S. Yamaguchi, Analysis of the dynamic characteristics of cross-flow heat exchangers with both fluids unmixed, Bull. JSME, vol. 21 (153), 1978, pp 479-485.
- [6] Hassan B.Kazemian , Development of an intelligent Fuzzy Controller, IEEE International Fuzzy Systems Conference. Vol.1, 2001, pp. 517-520.
- [7] Mann G. K.I., Hu B.G.Gosine R.G, Analysis of direct fuzzy PID controller structures, IEEE Trans on Systems, Man and Cybernetics. Vol.29, 1999, pp. 371-388.
- [8] M. Sugeno, Industrial applications of fuzzy control, Amsterdam, The Netherlands: Elsevier, 1985.
- [9] Li, H.X. & H. Gatland, Conventional fuzzy logic control and its enhancement, IEEE Transactions on Systems, Man and Cybernetics, 26(10), 1996, pp.791-797.
- [10] Jean-Jacques E. Slotine, Weiping Li, applied nonlinear control, Prentice-hall, Inc., London, 1991, pp. 278-282.
- [11] George K. I. Mann, Bao-Gang Hu, and Raymond G. Gosine, Two-level tuning of fuzzy PID controllers, IEEE transactions on systems, man, and cybernetics-part B: cybernetics, Vol. 31, No. 2001, pp. 263-269.
- [12] K. M. Hangos, J. Bokor, and G. Szederkényi, Analysis and control of nonlinear process control systems, Advanced Textbooks in Control and Signal Processing, 1st Edition, Ch. 4, Springer-Verlag London limited, 2004, pp. 55-61.

## EFFECT OF TOOL PIN PROFILES AND HEAT TREATMENT PROCESS IN THE FRICTION STIR WELDING OF AA 6061 ALUMINIUM ALLOY

P.Prasanna<sup>\*</sup>, Dr.Ch.Penchalayya<sup>\*\*</sup>, Dr.D.Anandamohana Rao<sup>\*\*\*</sup>

(Assistant professor, Department of Mechanical Engg, JNTUH College of Engg, Hyderabad-85,)\*

(Principal, ASR College of Engineering, Tanuku, West Godavari, Andhra Pradesh -534211, INDIA)\*\*

(Former Principal, JNTUK College of Engg, Kakinada, East Godavari, Andhra Pradesh -533004, INDIA)\*\*\*

**Abstract:** Friction stir linear welding (FSLW) uses a non consumable tool to generate frictional heat in the abutting surfaces. The welding parameters such as rotational speed, welding speed, axial force, tool tilt angle, etc., and tool pin profiles play a major role in deciding the joint properties. In this paper, an attempt has been made to study the effect of four different tool pin profiles on mechanical properties of AA 6061 aluminum alloy. Four different profiles have been used to fabricate the butt joints by keeping constant process parameters of tool rotational speed 1200RPM, welding speed 14mm/min and an axial force 7kN. Different heat treatment methods like annealing, normalizing and quenching have been applied on the joints and evaluation of the mechanical properties like tensile strength, percentage of elongation, hardness and microstructure in the friction stirring formation zone are evaluated. From this investigation, it is found that the hexagonal tool profile produces good tensile strength, percent of elongation in annealing and hardness in quenching process.

**Key words:** Friction stir linear welding; AA 6061Aluminium; Tool profiles; constant process parameters; Heat treatment;

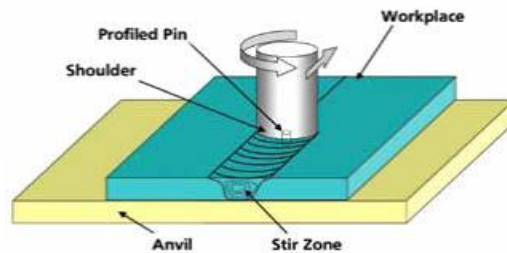
### I. INTRODUCTION

Friction Stir Welding (FSW) is a solid state welding process in which the relative motion between the tool and the work piece produces heat which makes the material of two edges being joined by plastic atomic diffusion. This method relies on the direct conversion of mechanical energy to thermal energy to form the weld without the application of heat from conventional source. The big difference between FSW and fusion welding (other than the lack of melting) is the ability to manipulate peak temperatures by choice of different welding parameters. Welding parameters, tool geometry, and joint design make use of considerable effect on the material flow pattern and temperature distribution, thereby influencing the micro structural evolution of material. Tensile strength is higher with lower weld speed. This indicates that lower range of weld speed is suitable for achieving maximum tensile strength. Friction stir welding of Al 6061- O condition increases the strength of the weld joint as compared to that of the parent material in O-condition were studied by Ahmed Khalid Hussain et. al[1]. Mechanical properties substantially improve during Post Weld Heat Treatment[2]. R.palanivel, et al have studied the influences of tool pin profiles on the mechanical and metallurgical properties of FSW of dissimilar alloys [3]. FSW offers a quality advantage that leads the welds strength and ductility either identical or better than that of the base metal alloy were proposed by Nayi Li1, et al.[4]. J. Adamowski a, M. Szkodo b have been studied on the rotational speed, welding speed and tool profiles are directly influenced on the tensile strength of FS welded joints [5]. The tensile strength of the FS welded is affected by the tool pin profile. The grain structure within the FSP is fine and equiaxed compared to TMAZ [5].P. V. Gopal Krishna, et. al are investigated in the friction drilling using HSS tool [6]. Cabello Munoz et al. investigated the micro structural and mechanical properties of friction stir welded and gas tungsten arc welded Al-Mg-Sc alloy and reported that the yield strength of friction stir welded and gas tungsten arc welded joints are decreased 20% and 50 % respectively compared to the base metal[7]. Optimization of FSW parameters in different conditions of base material and the

microstructures of the as-welded condition are compared with the post weld heat treated microstructures welded in annealed and T6 condition [9]. Elangovan K, Balasubramanian V, et. al are report on the influences of tool pin profile and axial force on the formation of Friction stir processing zone in AA6061 aluminium alloy [10]. Park HS, et.al have studied on microstructures and mechanical properties of AA 6061 alloy. FSW joints usually consist of four different regions. They are; (a) unaffected base metal; (b) heat affected zone (HAZ); (c) thermo mechanically affected zone (TMAZ); and (d) friction stir processed (FSP) zone[11]. The formation of above regions is influenced by the material flow behavior under the action of rotating non consumable tool. However the material flow behavior is predominantly affected by the FSW tool profiles, tool dimensions, and FSW process parameters [12]. Hence in this paper an attempt was made to study the influence of different tool profiles by keeping the constant process parameters as tool rotational speed, welding speed and axial force and also investigate the post weld heat treatment like annealing, normalizing and quenching are performed on FSW joints of AA 6061 aluminum alloy followed by tensile test and micro hardness measurements. Microstructure testing is also done by Scanning Electron microscope.

**II. EXPERIMENTAL DETAILS**

The specimens of the size of 200mmx100mmx5mm were machined from AA6061 aluminum alloy plates. The two plates of AA6061 aluminum alloy were Friction stir welded using four different tool profiles like taper cylindrical ,triangular , square and hexagonal made of high carbon high chromium steel. It comprises of 18mm shoulder dia, 6mm pin diameter and 4mm pin length under the constant process parameters of 1200 rpm, 14mm/min welding speed and 4kN axial force were applied in the butt configuration by using CNC vertical milling machine. The FSW procedure was based on the TWI procedure described in the patent by Thomas et al.(1991). The experimental set up is shown in Fig.1(a-d). The rotation of the tool resulted in stirring and mixing of material around the rotating pin and the linear movement of the tool moved the stirred material from the front to the back of the pin and finished the welding process. The insertion depth of the pin into the work pieces was associated with the pin height (length). The tool shoulder contacting the work piece surface depends on the insertion depth of the pin, which results in generation of welds with inner channel, surface groove, and excessive flash.



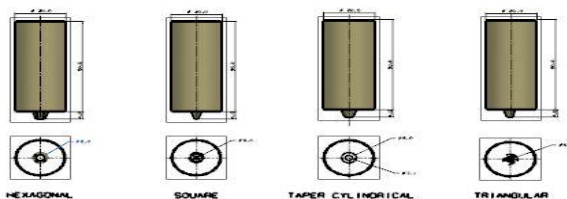
(a).Schematic diagram of FSW joint



(b). Photo of the CNC vertical machine



(c). Processing of the joint



(e). Fabricated joints



(d). FSW tool pin profiles

Fig.1. Experimental details

12 FSW butt joints were made by vertical conventional milling machine as shown in fig 1(e). Tensile tests were carried based on ASTM standard. The FSW joint plates were sawed into the dimension 200x20mm. The tensile tests were carried out by universal testing machine to find maximum loading and percentage of elongation. Percentage of elongation is defined as ratio of deformation to original length of 50mm. Hardness tests were carried out on Rockwell hardness machine at a force of 60kgf. The microstructure characterized by light microscopy, SEM in the base materials and in the weld nugget zone. Properties of aluminum alloy AA 6061 are given in the tables (1&2) and uncontrollable process parameters and tool dimensions are shown in the table (3).

Table1: Percentage of chemical composition AA 6061 alloy

Mg	Si	Fe	Cu	Zn	Ti	Mn	Cr	others	Al
0.8 -1.2	0.4-0.8	0.7	0.15-0.4	0.25	0.15	0.15	0.04-0.35	0.05	98.7

Table2. Mechanical and physical properties of AA 6061 alloy

Young's modulus (G Pa)	Yield strength (M Pa)	Ultimate tensile strength (M Pa)	% of elongation	Density (Kg/m <sup>3</sup> )	Hardness (BHN)	Melting range (° C)	Thermal conductivity (W/m-k)	Sp.heat (J/kg-°c)
68.9	235	283	26.4	68.9	107	582-652	167	0.896

Table 3: Selected welding parameters and tool dimensions

Process parameters	Values
Rotational speed (RPM)	1200 rpm
Welding speed (mm/min)	14mm/min
Axial force	7 kN
Tool material	High carbon High Chromium with 60-62 HRC
Tool dimensions	Shoulder dia 18mm, pin dia 6mm and pin length 5.5mm.
Tool pin profiles	Taper cylindrical
	Triangular
	Square
	Hexagonal

### III. INFLUENTIAL FACTORS OF WELD QUALITY

Factors affecting the weld quality include: tool material, tool configuration, rotation speed, welding speed, Axial force of tool on work pieces and the kind of work materials.

#### 3.1. Tool material and configuration:

The tool of FSW is composed of two parts: a tool body and a probe. The tool technology is the heart of friction stir welding process. The tool shape determines the heating, plastic flow and forging pattern of the plastic weld metal. The tool shape determines the weld size, welding speed and tool strength. The tool material determines the rate of friction heating, tool strength and working temperature, the latter ultimately determines which materials can be friction stir welded. Each of these tool technology aspects will be studied to try and establish a combination that will produce sound welds and the best tolerance to process parameters at the required working temperature. In some references, the shape of probe was a slanted British system screw, but in many references it was special [13-15].

The radius of the tool body's shoulder is almost three times of that of the probe. If the radius of the shoulder is too small, the friction heat is not enough to plasticize the materials beneath the shoulder. On the other hand, the friction heat may too large to make the temperature of the materials beneath the shoulder reach or exceed the melt point, consequently reduce the weld strength and raise the irregularity of the weld surface.

#### 3.2. Rotating speed of the tool:

According to the thermal analysis of FSW, the average frictional heat input ( $q$ ) per unit area and per unit time is given by Frigard [16]

$$q = \int_0^R \omega 2 \pi \mu P r^2 dr \quad (1)$$

where,  $q$  is the net power intensity (in Watts/m<sup>2</sup>),  $\omega$  the angular velocity (in rad/s),  $\mu$  the coefficient of friction,  $R$  the radius of the tool's shoulder (in meters),  $P$  the pressure across the interface (here assume constant). By substituting  $\omega = \frac{1}{30} \pi n$  into equal, we get:

$$q = \int_0^R \frac{2}{30} \pi^2 \mu P n r^2 dr = \frac{1}{45} \pi^2 \mu P n (R^3 - r^3) \quad (2)$$

where, n is the rotating speed of the tool (in rad/min).

From eqn 2, it is obvious that the rotating speed is one of the main factors affecting the frictional heat. If the rotating speed is too low, the frictional heat is not enough to induce plasticized flow, the metal in the weld cannot diffuse and recrystallize, and there are holes in the weld. Along with an increase of the rotating speed, the frictional heat increases, the plasticized layer increase from top to the underside, the holes in the weld become smaller. When the rotating speed reaches a certain number, the holes in the weld becomes tightness. But if the rotating speed is too high, the temperature of materials beneath the tool's shoulder and around the probe will excess the melt point, and the weld is no long a solid-state joint.

### 3.3 Welding velocity:

From equation 2, we can understand that the net power intensity is constant only when the structure of the weld tool and the rotating speed are confirmed. So, when the welding velocity is too small, the frictional heat makes the temperature in the weld too high (may reach or excess the melt point), the materials will be porous, inducing fluidification crack, and the weld surface will be irregular. On the other hand, when the welding velocity is too large, the frictional heat is not enough to plasticize the materials beneath the tool's shoulder and around the probe, the work pieces can't be welded[17-19].

### 3.4 Axial force of tool on the work pieces:

The press force of tool on work pieces affects the contact state, whereas the contact state affects the forming of weld. When the press force is not enough, the surface metal of the weld "floats" upward and overflows the surface of work pieces, resulting in holes at the bottom of the welding. When the press force is too large, the frictional force between the tool's shoulder and the work pieces's surface increases, the tool's shoulder will cohere with the materials of work pieces and there will be flashes and burs on the weld face.

## IV. HEAT TREATMENT METHODS

### 4.1. Annealing Process:

In this method, The butt weld joints are heated in the muffle furnace up to 580<sup>0</sup> C and holding the same temperature for a period of 2-3 hrs in order to get the homogeneous structure and then cooled in the furnace to attain the room temperature .

### 4.2. Normalizing Process:

In this method, The butt weld joints are heated in the muffle furnace up to 580<sup>0</sup> C and holding the same temperature for a period of 2-3 hrs in order to get the homogeneous structure and then cooled in the air to attain the room temperature .

### 4.3. Hardening Process:

In this method, The butt weld joints are heated in the muffle furnace up to 580<sup>0</sup> C and holding the same temperature for a period of 2-3 hrs in order to get the homogeneous structure and then cooled in the water to attain the room temperature .

## V. MECHANICAL TESTS

From each of the heat treatment processes, the specimens are taken and tested for mechanical properties like tensile test, Vickers hardness test and microstructure.

### 5.1. Tensile test:

American Society for Testing of Materials (ASTM) guidelines are followed for preparing the test specimens. Tensile test has been carried out in 20 kN, Universal Testing Machine as shown in fig 2. The specimen finally fails after necking which occurs in the friction stirred region (FSP).



Fig 2: Universal Testing machine

**5.2. Hardness test:**

Rockwell hardness testing machine has been employed for measuring the hardness across the joint and perpendicular to the joint with 60 kg load. The hardness have been evaluated for Taper cylindrical, triangular , square and hexagonal tool pin as shown in fig(3).



Fig 3: Rockwell Hardness Tester

**5.3. Microstructure:**

Samples for microstructure observations were cut from both the FSW plates. The cut samples, 0.5 in. square in cross-section, were mounted in Bakelite and then dry ground on progressively finer grades of silicon carbide impregnated emery paper. Fine polishing to a perfect mirror-like finish of the surface was achieved using disc polishing kerosene solution as the lubricant.

The polished aluminum alloy sample of Plates was etched using Keller's reagent (a solution mixture of 1 drop hydrofluoric acid, 25ml concentrated nitric acid, 25ml hydrochloric acid and 25ml methanol). The etched surface of each sample containing the weld region was observed in an optical microscope and photographed using a bright field illumination (AVER CAP software) technique as shown in fig(4).

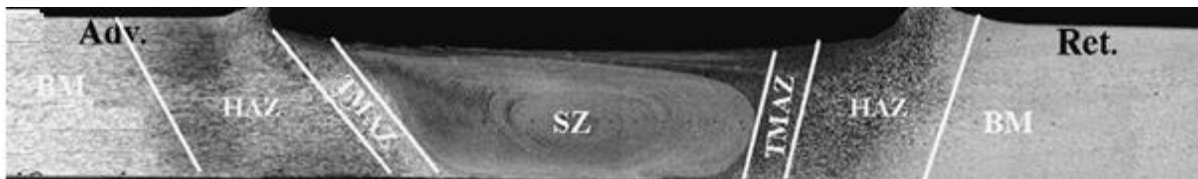


Fig.4 Typical macrograph showing various regions of the FS welded plates of AA 6061 alloy on AS, RS.

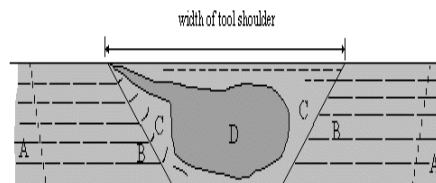


Fig 5. Schematic illustration diagram of various friction stirred zones of AA 6061 alloy

**A:** Unaffected material **B:** Heat Affected zone (HAZ) **C:** Thermo-Mechanically Affected Zone (TMAZ)  
**D:** Weld Nugget (Part of thermo-mechanically affected zone)(SZ)

Unaffected material or parent metal (A): This is material remote from the weld, which has not been deformed, and which although it may have experienced a thermal cycle from the weld is not affected by the heat in terms of microstructure or mechanical properties.

Heat affected zone (HAZ) (B): This is region which will lie closer to the weld centre; the material has experienced a thermal cycle which has modified the microstructure and/or the mechanical properties. However, there is no plastic deformation occurring in this area, which is referred to as the heat affected zone or thermal affected zone. Thermo-mechanically affected zone (TMAZ) (C): In this region, the material has been plastically deformed by the friction stir welding tool, and the heat from the process will also have exerted some influence on the material. However, subsequent work on other materials has shown that aluminum behaves in a different manner to most other materials, in that it can be extensively deformed at high temperature without

recrystallisation. In other materials, the distinct recrystallised region (the nugget) is absent, and the whole of the TMAZ appears to be recrystallised. This is certainly true of materials which have no thermally induced phase transformation which will in itself induce recrystallisation without strain. Weld Nugget or Stir Zone (SZ): The recrystallised area in the TMAZ in aluminum alloys has traditionally been called the nugget. It has been suggested that the area immediately below the tool shoulder (which is clearly part of the TMAZ) should be given a separate category, as the grain structure is often different here. The microstructure here is determined by rubbing by the rear face of the shoulder, and the material may have cooled below its maximum.

**VI. RESULTS AND DISCUSSIONS:**

Successfully joints were obtained by FSW processes for the all the process parameters used in the investigation. Typical example of FS welds is shown in Fig. (3), in which the upper and bottom surfaces of the weld are seen at the process condition of; 1200 rpm rotational speed, 14mm/min of welding speed, 7kN axial force. Visual and macroscopic inspection of the weld surfaces has showed no observed superficial macroscopic defects. Usually, the FSW process leaves a pin hole at the weld end, as can be seen in Fig. (3.a), and the design of the weld is done in such a way that the part with the hole is cut and not used for further processes. The mechanical properties of AA 6061 alloy FSW joints of such ultimate tensile strength, percentage of elongation and hardness are evaluated. At each condition three specimens are tested and average of the results of three specimens is presented in the table 4.

**6.1. Effect of Tool pin profiles on Ultimate tensile strength for different heat treatment process**

Table 4: Mechanical properties obtained for Taper Cylindrical tool pin profile

Heat treatment Process	Taper cylindrical		Triangular		Square		Hexagonal	
	UTS (N/mm <sup>2</sup> )	% Elongation						
Annealing	145	28.34	170	26.56	198	24.78	210	20.9
Normalizing	130	18.8	145	20.3	187	22.5	195	24.3
Quenching (water)	120	9.6	125	9.5	124	8.9	130	10.3

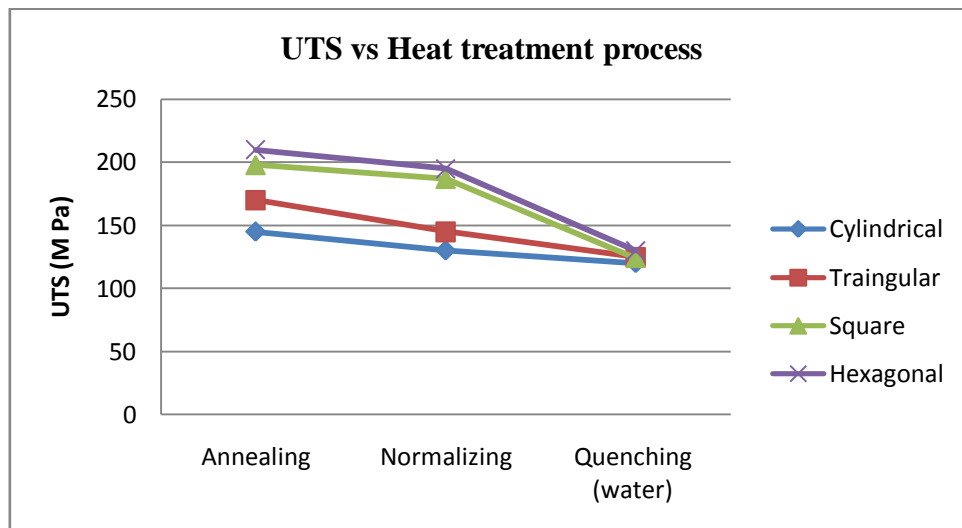


Fig.6: Effect of tool profile on Ultimate tensile strength for different heat treatment process

Fig 6. Shows that the variation of UTS for various profiles with respect to different heat treatment processes of annealing, normalizing and quenching. It can be inferred that tool pin profile has influenced on the ultimate tensile strength and percentage of elongation. Of the four profiles, it is observed that the maximum ultimate tensile strength occurred for hexagonal tool pin profile for annealed condition compared to the other profiles due to the grain refinement of the FSW joint. Similarly square pin profile also showing almost matching

the properties of the hexagonal tool profile. The taper cylindrical pin profile tool exhibited inferior tensile properties compared to the counters. The percentage of elongation is maximum for the taper cylindrical pin profile for annealing condition. Similarly the triangular pin profile showed the matching properties of taper cylindrical pin profile. It is found that FSW softens the joints of the present alloy because the strengthening precipitates dissolved and grew during the weld thermal cycle which results degradation of the mechanical properties.

**6.2: Effect of Tool pin profiles on microstructure for heat treatment process:**

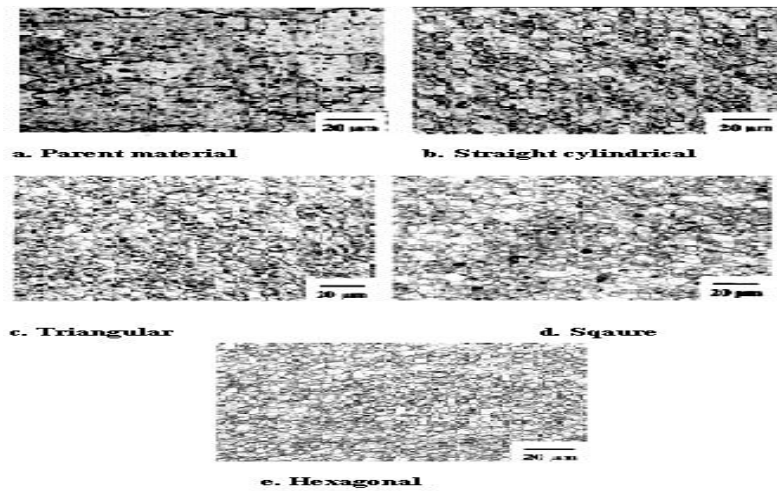


Fig 7(a-e): Microstructures showing different tool profiles at weld zone. ( 400x ). Dark particles of Mg<sub>2</sub>Si are embedded in a matrix of Aluminum rich solid solution etched by Keller's reagent

From Fig 7(a), it is shown that the base metal microstructure basically consists of elongated grains and the strengthening particles are uniformly distributed throughout the matrix. Few considerable variations in grain size and distribution of strengthening particles Mg<sub>2</sub>Si are clearly visible in micrographs. From fig 7(b), The elongated grains are changed into equi-axed grains from the base metal microstructure in the Stirred zone (SZ) friction stirred process region, irrespective of tool pin profiles used to fabricate the joints. Due to the absence of pulsating action and insufficient working of the plasticized material, the grain size is comparatively higher in the SZ than the base metal produced by taper cylindrical pin. From fig 7(c-e), Pins with flat faces like triangular, square and hexagonal produced the pulsating stirring action and caused reduction in grain size and homogenous redistribution of second phase particles throughout the matrix at Nugget zone. It is observed that the more redistribution of the second phase particles in the matrix and reduction grain size occurred in hexagonal tool pin profile with annealing process resulting in better tensile strength.

**6.3. Effect of Tool pin profiles on Hardness for different heat treatment process**

Table 5(a): Hardness varying with Taper Cylindrical tool pin profile

Distance from weld center, mm	Vickers's Hardness, (RV)		
	Annealing	Normalizing	Quenching (water)
-40(AS)	78	82	84
-30(AS)	75	80	85
-20(AS)	74	79	79
-10(AS)	70	78	78
0( NZ)	67	73	77
10(RS)	70	79	73
20(RS)	74	80	73
30(RS)	77	81	84
40(RS)	79	82	85

Table 5(b): Hardness varying with Triangular tool pin profile

Distance from weld center, mm	Rock well Hardness, (HBN)		
	Annealing	Normalizing	Quenching (water)
-40(AS)	80	82	94
-30(AS)	82	85	93
-20(AS)	81	70	90
-10(AS)	78	68	88
0( NZ)	74	65	84
10(RS)	79	67	89
20(RS)	80	73	91
30(RS)	81	84	92
40(RS)	80	85	94

Table 5(c): Hardness varying with Square tool pin profile

Distance from weld center, mm	Rock well Hardness, (HBN)		
	Annealing	Normalizing	Quenching (water)
-40(AS)	89	94	104
-30(AS)	87	92	102
-20(AS)	80	89	98
-10(AS)	70	88	95
0( NZ)	74	82	90
10(RS)	73	89.5	92
20(RS)	86	90	96
30(RS)	89	92	100
40(RS)	91	93	103

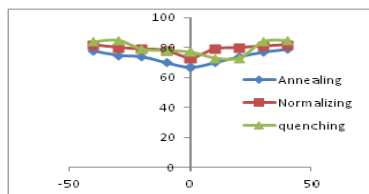
Table 5(d): Hardness varying with Hexagonal tool pin profile

Distance from weld center, mm	Rock well Hardness, (HBN)		
	Annealing	Normalizing	Quenching (water)
-40(AS)	92	98	103
-30(AS)	93	97	101
-20(AS)	89	95	100
-10(AS)	83	92	98
0( NZ)	80	90	94
10(RS)	87	92	99
20(RS)	92	94	102
30(RS)	92	96	101
40(RS)	91	97	103

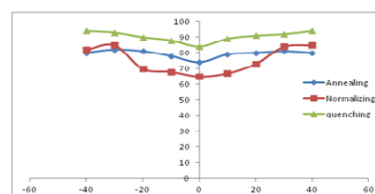
AS: Advanced side

RS: Retreating side

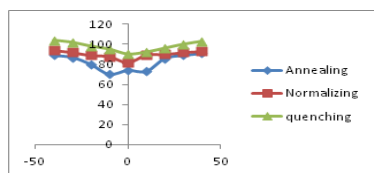
NS : Nugget Zone



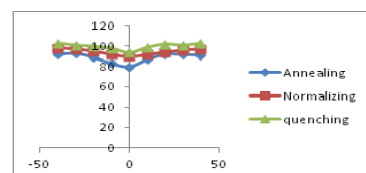
a. Taper cylindrical



b. Triangular



c. Square



d. Hexagonal

Fig 8(a-d): The Hardness distribution and comparison at various zones of different profiles with different heat treatment Process.

From fig 8(a-d), it is shown that the hardness values are decreasing from advanced side to Nugget zone and further it is increasing till retreating side for different heat treatments like annealing, normalizing and quenching varies with respect to different tool pin profiles. It is observed that the maximum hardness occurs at quenching process with hexagonal tool profile which gave the fine grain structure and more  $Mg_2Si$  particles distributed in the aluminum alloy.

## VII. CONCLUSIONS:

The joints fabricated using different tool pin profiles like Taper cylindrical, triangular, square and hexagonal tool with a rotational speed of 1200RPM, weld speed of 14mm/min and axial force of 7kN. The following important conclusions were made for the present investigation.

1. Of the four tool profiles, The maximum tensile strength and % of elongation of 210M Pa and 20.9 respectively was observed on Hexagonal pin profile tool with annealing process.
2. The tensile strength and percent of elongation of the hexagonal tool profile with annealing process has reached about 90% and 80% respectively of the parent metal.
3. The hardness of FSP zone fabricated using hexagonal profile tool with quenching is higher compared to other type of tool profiles.
4. The microstructure of FSP region contained fine equiaxed grains and very fine uniformly distributed strengthening precipitates( $Mg_2Si$ ) throughout the matrix of hexagonal pin profile. This may be the reason for superior tensile properties of these joints.

## REFERENCES:

- [1] Ahmed Khalid Hussain et. al. "Evaluations of parameters of FSW for AA6351" International journal of engineering science and technology vol 2 (10), 2010, 5977-5984.
- [2] Rhodes CG, Mahoney MW, Bingel WH. 1997. Micro structural changes determining joint strength in friction stir welding of aluminum alloys. Scripta Mater. R.palanivel, Dr.P.Koshy Mathews , Dr.N.murugan "Influences of tool pin profiles on the mechanical and metallurgical properties of FSW of dissimilar alloys" International Journal of Engineering Science and Technology Vol. 2(6), 2010, 2109-2115.
- [3] Naiyi Li1, Tsung-Yu Pan1, Ronald P. Cooper1, Dan Q.Houston1, Zhili Feng2 and Michael L. Santella2 "FSW of magnesium alloy AM60" 19Magnesium Technology 2004 Edited by Alan A. Luo TMS (The Minerals, Metals & Materials Society), 2004.J. Adamowski a, M. Szkodo b "Friction Stir Welds (FSW) of aluminum alloy AW6082-T6 GSE", Ansaldo Energia, Via Lorenzi 8,16100 Genoa, Italy VOLUME 20 ISSUES 1-2 January-February 2007.P. V. Gopal Krishna, K. Kishore, and V. V. Satyanarayana "some investigation in friction drilling using HSS tool" ARPN Journal of Engineering and Applied Sciences VOL.5, NO. 3, March 2010.
- [4] Munoz C, Ruckert G, Huneau B, Sauvage X, Marya S (2004) Comparison of TIG welded and friction stir welded Al-4.5 Mg-0.26 Sc alloy. J Mater Process Technol 152:97-105
- [5] S.K. Chionopoulos, CH.I. Sarafoglou, D.I. Pantelis, V.J.Papazoglou "Effect of tool pin and welding parameters on Friction Stir Welded (FSW) marine aluminium alloys" Proceedings of the 3rd International Conference on Manufacturing Engineering (ICMEN), 1-3 October 2008.
- [6] Indira Rani M., Marpu R. N. and A. C. S. Kumar, "A study of process parameters of friction stir welded AA 6061 aluminum alloy in O and T6 conditions" ARPN Journal of Engineering and Applied Sciences, Vol. 6, No.2, February 2011.
- [7] Elangovan K, Balasubramanian V, Valliappan M (2007) Influences of tool pin profile and axial force on the formation of Friction stir processing zone in AA6061 aluminium alloy. Int J Adv Manuf Technol (in press). DOI 10.1007/s00170-007-1100-2
- [8] Park HS, Kimura T, Murakami T, Nagano Y, Natka K, Ushio M. 2004. Microstructures and mechanical 65 Vol. 6, No. 2, Feb 2011 ISSN 1819-6608 ARPN Journal of Engineering and Applied Sciences ©2006-2011 Asian Research Publishing Network (ARPN).
- [9] Xie GM, Ma ZY, Geng L. 2007. Development of a fine grained microstructure and the properties of a nugget zone in friction stir welded pure copper. Scripta Mater: 73-76.
- [10] Campbell G, Stotler.T " Friction stir welding of armor grade aluminum plate" welding journal (MIAMI,FLA)-1999, 78[12]:45-47
- [11] Thomas W M, Nicholas E D. Friction Stir Welding for the Transportation Industries. Materails and design, 1997, 18(4-6) :269-273.
- [12] Sato Y S,Kokawa H, et al.. Microstructure in the Friction-stir Weld of an Aluminum Alloy. Metallurgical and material Transactions A: Physical Metallurgy and Materials Science,2001,32(4) :941-948
- [13] Frigaard et al O.T.1988. "Modelling of the heat flow phenomenon in friction stir welding of aluminum alloys. Proceedings of the seventh international conference joints in aluminum", INALCO 98, Cambridge, UK, April 15-17.,pp.1189-1200.
- [14] Steward W W. Welding of Airframes Using Friction ,Stir. Air &Space Furop ,2001,3(3/4) :64-66
- [15] Joelj D. The Friction Stir Welding Advantage. Welding Journal,2001,80(5) :30-34
- [16] Li Y, TfiUo E A, Murr L E. Friction-stir Welding of Aluminum Alloy 2024 to Silver. Journal of Material Science Letters, 2000,19(12) : 1047-1051

## Comparative Study of The Effects Of Sawdust From Two Species Of Hard Wood And Soft Wood As Seeding Materials On Biogas Production

Oluwaleye, Iyiola Olusola<sup>1</sup> and Awogbemi, Omojola<sup>2</sup>

Department of Mechanical Engineering, Ekiti State University, Ado Ekiti, Nigeria

**Abstract:** The effects of two varieties of sawdust from hard and soft woods as seeding materials on biogas yield were investigated. The substrates for the experiment in an anaerobic laboratory digester are cow dung and cassava peels. The hard woods are Mahogany and Iroko, while the soft woods are Obeche and Araba. The experimental set-ups were sub-divided into four groups of digesters. Each group was made up of four digesters seeded with sawdust from the wood types in the following percentages: 33%, 27%, 20%, and 11%. 200g of cow dung and cassava peels were mixed with 120cm<sup>3</sup> of distilled water in each digester. The seeding materials in different percentages were added and mixed thoroughly and the biogas produced was recorded at a regular interval of 4 days for an hydraulic retention time of 40 days. The volume of biogas produced ranged from 60cm<sup>3</sup> to 2800cm<sup>3</sup>. In all the experiments, the biogas yield decreases with decrease in percentage of sawdust seeding materials. Digester A in group I with 33% of mahogany has the largest biogas yield of 329.63 cm<sup>3</sup>/day while digester H in Group II with 11% Iroko sawdust has the least yield of 61.63 cm<sup>3</sup>/day.

**Keywords:** Biogas, Hard wood, Soft wood, Anaerobic digester, Media content.

### I. INTRODUCTION

Society is today confronted with dwindling and depletion sources of fossil fuels and chemical feedstock, and battling with the proliferation of wastes generated by municipalities, agriculture and industries. The conversion techniques of renewable resources or wastes to useful chemicals and fuels by microbial fermentation through a reactor signifies a tremendous challenge for engineers in global technological stance, and the future ahead with respect to energy demand.

Anaerobic biodegradation of cellulosic materials is a biological engineering process [1] in which a methane –rich gas (biogas) is produced and slurry that is of proven value as fertilizer and animal feed is left as a residue. Several works have been undertaken in improving biogas yield such as the pretreatment of waste feedstock [2]. These pretreatments include: preheating, milling, chemical treatment with sodium hydroxide (NaOH) and other components. One of the major and relevant components of the process is the micro –organisms that are responsible for the enzymatic or catalytic breakdown of the feedstock and the subsequent conversion to methane (CH<sub>4</sub>), carbon dioxide (CO<sub>2</sub>) and traces of hydrogen (H<sub>2</sub>), nitrogen (N<sub>2</sub>) and hydrogen sulphide (H<sub>2</sub>S).

Sawdusts are produced as a small discontinuous chips or small fragments of wood during sawing of logs of timber into marketable sizes. The chips flow from the cutting edges of the saw blade to the floor during sawing operation, hence its name Sawdust has hitherto been classified as a waste and a nuisance to man and its environment, but in recent years, researches have shown that sawdusts can be used in the production of biogas, packaging fillers, as lagging materials etc [3,4]. The use of media materials (sawdust as seeding materials) to ensure a higher concentration of these micro- organisms would accelerate the rate of biogas yield by ensuring the passage of the three phases of gas production throughout the digester concurrently. This affects the start-up characteristics of the process positively by acting as the seeding micro-organism in different locations during feed stocks reloading [5]. The quantity and quality of media materials [6] such as synthetic materials, wood species, limestones etc to be expressed in percentage of total volume appropriateness especially since a higher percentage symbolizes a lower input of cellulosic material as feedstock, which in turn affects biogas yield.

Generally, the organic matter must be highly degradable to achieve a large yielding gas. Conversely, lower gas production rates would result from less biodegradable wastes [7]. Hence, it is paramount to determine an optimal percentage of media material. The effects of media material in biogas production have been well investigated by researchers in Nigeria and other parts of the world and are well recorded in literature [8]. Wastes like manure, agricultural crops, food wastes, urban refuse, industrial wastes, logging and manufacturing residues have been found to have biogas generation potentials [9].

This work investigates the effects of seeding varying quantities of two hardwoods and soft woods species on biogas yield using cowdung and cassava peels as feedstocks. The two hard wood species are Khaya species [Meliaceae family] known as Mahogany and *Milicia excelsa* [moraceae family] known as Iroko in local dialect. The two soft wood species are *Triplochiton scleroxylon* (Obeche) and *Cieba pentandra* [bombacaceae family] (Araba in local dialect).

## II. MATERIALS AND METHOD

Freshly voided cow dung was collected from the main abattoir in Ado-Ekiti while fresh cassava peels were collected from a gaari processing factory at the Onigari area of Ado Ekiti. The cassava peels were sundried and ground with the aid of a clean mortar and pestle. Sawdust from two hardwood species: Mahogany and Iroko and soft wood species: obeche and araba were collected from the Ewenla sawmill in Ado Ekiti and were used as seeding material to determine their effects on biogas generation. These four species were chosen because of their cellulose concentration and availability in the local environment. The Cow dung, Cassava peels, and sawdust samples were screened for unwanted foreign material like wood, stone, metal, bone, etc.

Sixteen digesters divided into four groups of four digesters were set up in the laboratory. The digesters were labelled A to P and each of them contains 200g of both cow dung (CD) and cassava peels (CP) in equal proportion. They were mixed with 120 cm<sup>3</sup> of sterile distilled water. Each group were seeded with varying quantity of Mahogany, Iroko, Obeche, Araba sawdust respectively.

Group I digesters, labelled A to D were seeded with 200g, 150g, 100g, and 50g of Mahogany wood (MW) sawdust respectively while group II digesters, labelled E to H were seeded with 200g, 150g, 100g, and 50g of Iroko wood sawdust respectively. Groups III and IV consisted of digesters labelled (I-L) and (M-P) respectively and were seeded with the same quantity of Obeche and Araba sawdust.

The resulting slurry was thereafter fed into the airtight digester bottles with the aid of a funnel. Each digester bottle was connected to a measuring cylinder inverted over acidified water in a plastic bowl as shown in Fig. 1. The cylinder was used as a measuring scale as well as gas collector. The acidified water was prepared by adding 0.05ml sulphuric acid (H<sub>2</sub>SO<sub>4</sub>) to 18.4w of water. This acidified water solution was used to prevent the dissolution of the biogas generated into the water. The digesters were corked to generate an anaerobic condition. The volumes of biogas produced were recorded at a specified interval of 4days for an Hydraulic Retention Time (HRT) of 40days.

In the course of the experiment, the average ambient temperature was 35°C while the pH varied between 6 and 8. The digester bottles were shaken daily to prevent the settling of the bacteria at the digester base and maintaining firm contact between bacteria and manure properly, prevent surface scum formation of the slurry in the digester, and facilitate the generation of biogas.

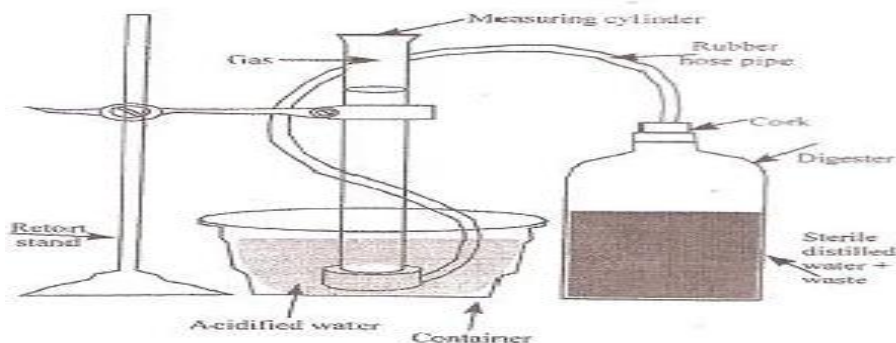


Figure 1: Experimental set up for biogas production.

## III. RESULTS AND DISCUSSIONS

The quantities of biogas generated from all the digesters (A-P) were recorded every four days for an HRT of 40days and tabulated as shown in Tables 1 and 2. Table 1 shows the biogas production every four days for a total of 40 days for digesters group I and II while Table 2 depicts the biogas production from digesters in group III and IV.

Table 1: The Table of biogas generations in cm<sup>3</sup> for digesters in groups I and II

Period (Days)	Group I digesters (Mahogany sawdust)				Group II digesters (Iroko sawdust)			
	A (cm <sup>3</sup> )	B (cm <sup>3</sup> )	C (cm <sup>3</sup> )	D (cm <sup>3</sup> )	E (cm <sup>3</sup> )	F (cm <sup>3</sup> )	G (cm <sup>3</sup> )	H (cm <sup>3</sup> )
1-4	615	490	460	400	260	200	240	85
5-8	1750	1190	995	799	600	320	360	125
9-12	2215	1885	1220	920	1000	530	700	290
13-16	2800	2480	1820	1145	1130	875	740	710
17-20	1480	1260	1710	950	800	510	345	520
21-24	1100	950	880	845	790	425	280	295
25-28	1025	920	850	715	760	415	215	200
29-32	980	745	850	610	675	350	170	100
33-36	690	420	760	300	260	320	140	80
37-40	530	395	300	280	170	120	100	60
Total	13185	10735	9845	6964	6445	4065	3290	2465
Mean (cm <sup>3</sup> /day)	329.62	268.38	246.13	174.1	161.13	101.63	82.25	61.63

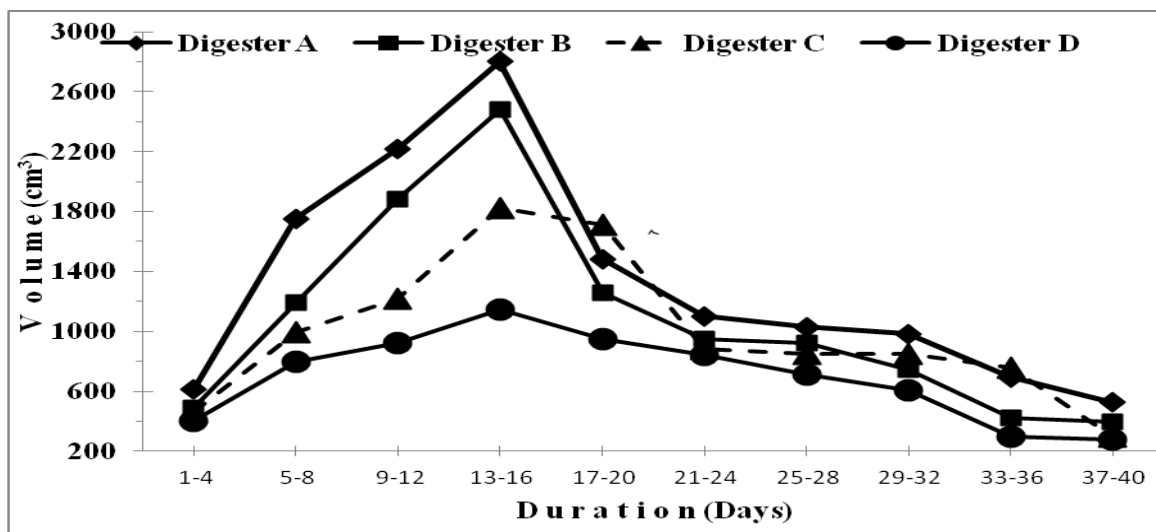


Figure 2: Daily production of biogas in Digesters (A-D) seeded with hardwood (Mahogany) sawdust

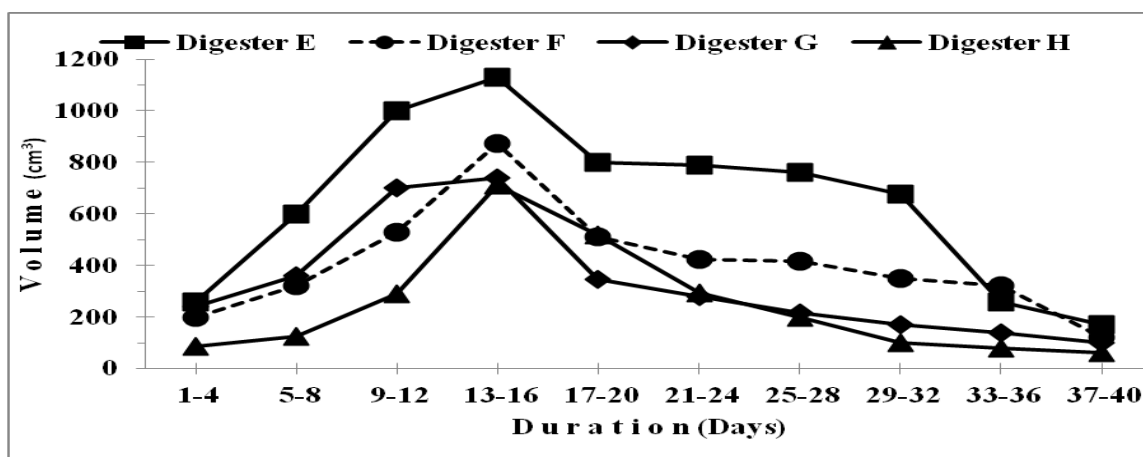


Figure 3: Daily production of biogas in Digesters (E-H) seeded with hardwood (Iroko) sawdust

The result shown above revealed that, the rate of biogas produced was solely dependent on the quantity of seeding media material in line with Adeyemo S.B. and Adeyanju A.A. [10]. Of the four digesters in group I, digester A (with 200g of mahogany sawdust) produced the highest quantity of biogas compared with digesters B, C, D which are seeded with 150g, 100g, and 50g of mahogany respectively as shown in Table 1. The lowest production of gas was recorded between day 37-40 for all the digesters while the peak period of gas production

was between day 13-16, where digesters A,B,C, and D recorded 2,800cm<sup>3</sup>, 2,480cm<sup>3</sup>, 1,820cm<sup>3</sup> and 1,1450cm<sup>3</sup> respectively as shown in Fig. 2. With the presence of the media material having higher moisture content could be explained by the fact that, the biodegradation process commenced within 48hours which is in line with that of Itodo I.N, Lucas E.B. and Kucha E.I [11]. The total volume of gas produced within 40days of digestion by digesters A, B, C, and D was 13,185cm<sup>3</sup>, 10,735cm<sup>3</sup>, 9,845cm<sup>3</sup> and 6,964cm<sup>3</sup> respectively.

The rate of biogas produced appeared highest in digester A followed respectively by digesters B, C, and D and this is due to the variation in the media content of the mahogany wood. It was noticed that, production of gas in all the digesters lasted for 40days and there was no deterioration noticed in the wood samples used. This may be due primarily to the abundant presence of lignin (which is not readily biodegradable by anaerobic organisms) in the wood samples.

For group II digesters seeded with varying quantity of Iroko sawdust, digester E with highest quantity of iroko sawdust (200g) was the most productive followed by digesters F, G, and H seeded with 150g, 100g, and 50g respectively in that order. Group II digesters also followed the same pattern of yield as group I digesters with the highest yield occurring between 13-16days as shown in Fig. 3. The mean daily yield was 161.13cm<sup>3</sup>, 101.63cm<sup>3</sup>, 82.25cm<sup>3</sup>, and 61.63cm<sup>3</sup> for digesters E, F, G and H respectively as shown in Table 1 and Fig. 4.

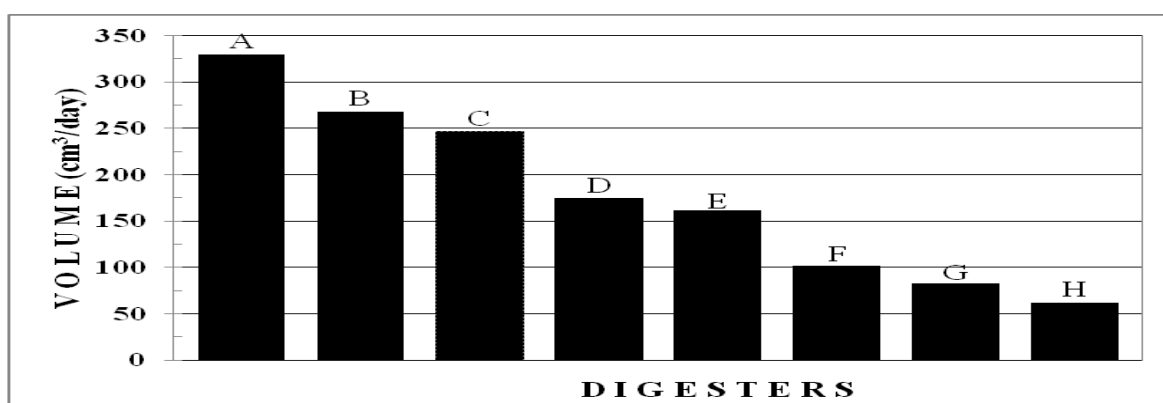


Figure 4: Comparative mean volumetric production of biogas/day in Digesters (A-H) seeded with hardwood sawdust

From Fig. 4, it is clear that the mean daily yield of each digester is directly proportional to the quantity of seeding material used. Also, digesters seeded with mahogany sawdust were more productive than those seeded with iroko sawdust even though mahogany and iroko woods are both hard wood species. Mahogany sawdust exhibit great biogas yield so much that the digester D seeded with 50g of mahogany sawdust yields more than digester E which was seeded with 200g of iroko sawdust. This shows that wood species affects biogas yield more than the quantity of seeding material.

Table 2: The Table of biogas generations in cm<sup>3</sup> for digesters in groups III and IV

Period (Days)	Group III digesters (Obeche sawdust)				Group IV digesters (Araba sawdust)			
	I (cm <sup>3</sup> )	J (cm <sup>3</sup> )	K (cm <sup>3</sup> )	L (cm <sup>3</sup> )	M (cm <sup>3</sup> )	N (cm <sup>3</sup> )	O (cm <sup>3</sup> )	P (cm <sup>3</sup> )
1-4	400	340	320	290	280	200	150	100
5-8	1200	1090	900	680	800	700	440	300
9-12	2050	1400	1200	890	1140	970	800	780
13-16	2400	2010	1750	1000	1200	1040	900	790
17-20	1300	1100	1000	790	930	840	650	450
21-24	940	900	800	510	790	610	450	290
25-28	600	550	500	400	690	400	320	230
29-32	550	450	400	350	640	380	300	230
33-36	480	400	350	230	320	295	250	180
37-40	330	310	240	200	200	170	120	80
Total	10250	8550	7460	5340	6990	5605	4380	3430
Mean (cm <sup>3</sup> /day)	256.25	213.75	186.5	133.5	174.75	140.13	109.5	85.75

Groups III and IV digesters are both seeded with soft woods, while group III digesters were seeded with Obeche, group IV digesters were seeded with araba sawdust. The production patterns were also similar to those exhibited by groups I and II digesters which are seeded with hard wood species.

For group III digesters, digester I which was seeded with 200g obeche sawdust was the most productive followed by digesters J, K, and L which were seeded with 150g, 100g, and 50g respectively. The highest yield occurred during the 13-16 days while the least yields were recorded in 37-40 days as shown in Table 2 and Fig. 5. Similar trends were also witnessed in group IV digesters seeded with varying quantity of araba sawdust where digester M seeded with 200g of araba sawdust was the most productive when compared with digesters N, O and P which are seeded with 150g, 100g and 50g of araba sawdust respectively. Fig. 6 reveals that the peak biogas yields were recorded between 13-16 days while the least were recorded between 37-40 days.

The mean daily production was highest in digester I ( $256.25\text{cm}^3$ ) and was followed by digester J ( $213.75\text{cm}^3$ ), digester K ( $186.5\text{cm}^3$ ), and digester L ( $133.5\text{cm}^3$ ) in that order for group III digesters. The average daily production for group IV digesters was highest in digester M ( $174.75\text{cm}^3$ ) followed by digester N ( $140.13\text{cm}^3$ ), digester O ( $109.5\text{cm}^3$ ) and digester P ( $85.75\text{cm}^3$ ) in that order as shown in Fig. 7.

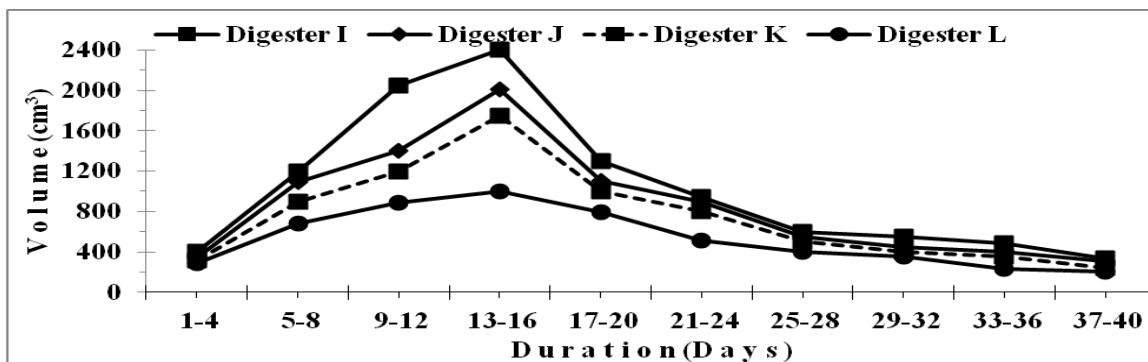


Figure 5: Daily production of biogas in Digesters (I-L) seeded with softwood (Obeche) sawdust

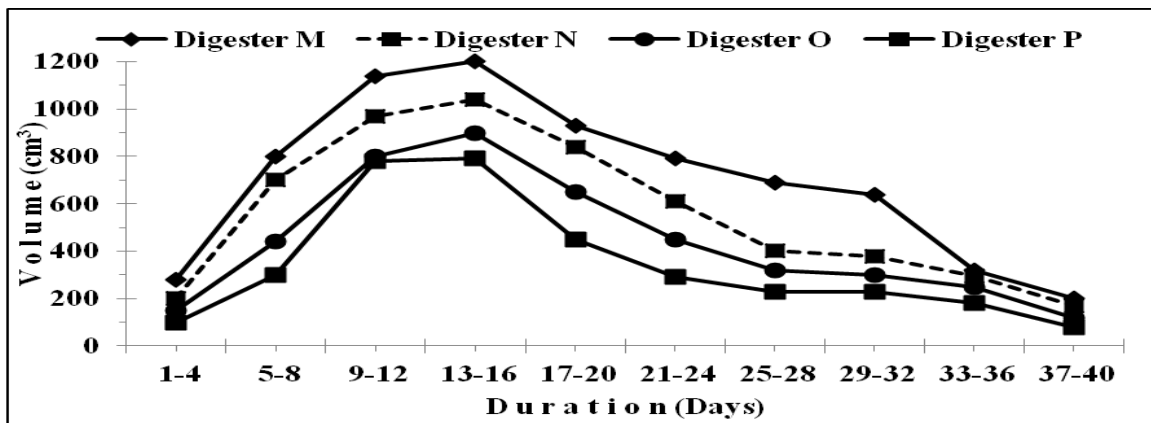


Figure 6: Daily production of biogas in Digesters (M-P) seeded with softwood (Araba) sawdust

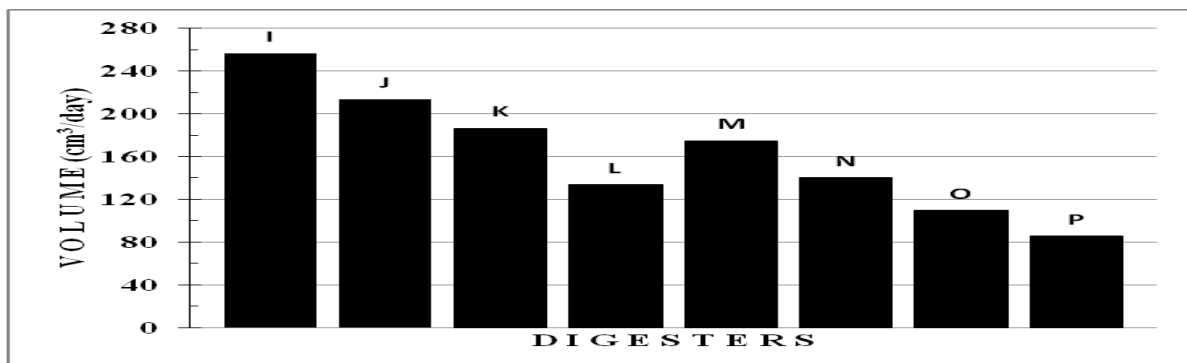


Figure 7: Comparative mean volumetric production of biogas/day in Digesters (I-P) seeded with softwoods sawdust

Unlike what happened in the case of hardwood where digester D that was seeded with 50g of mahogany sawdust yielded more biogas/day than digester E seeded with 200g of iroko sawdust (Fig. 4), digester L seeded with 50g of Obeche sawdust produced less biogas/day than digester M seeded with 200g araba sawdust (Fig. 7).

Comparatively, of the four digesters seeded with 200g of sawdust, digester A (seeded with 200g mahogany hardwood sawdust) is the most productive followed by digester I (seeded with 200g obeche softwood sawdust), digester M (seeded with 200g araba softwood sawdust), and digester E (seeded with 200g iroko hardwood sawdust) in that order. Also of all the sixteen digesters digester A was the most productive generating  $329.62\text{cm}^3$  in 40 days while digester P generated the least volume of biogas of  $3430\text{cm}^3$  during the same period.

#### IV. CONCLUSION

The tremendous increasing costs of conventional fuels in the urban areas necessitate the exploration of other energy sources. Biogas could be produced from animal wastes, wood wastes and other bio-wastes to substitute for fossils fuels. The search for alternative energy sources such as biogas should be intensified so that, ecological disasters like deforestation could be solved.

This research work has shown an increase production of biogas through the use of varying quantities of seeding materials (varieties of wood species). The various concentration of the two hard woods (mahogany and Iroko) exhibits good and better characteristics in accelerating biogas yield than the two other soft woods (Obeche and Araba). However, mahogany wood had distinguished its media potential unique content in generating the highest rate of biogas production among other tested wood species. More researches should be carried out to determine the exact quantity of mahogany sawdust that will guarantee optimum biogas yield.

Hence, while the quantity of seeding material can increase biogas yield, the type and quality of seeding material can also contribute significantly to the production capacity.

#### V. REFERENCES

- [1] S.B Adeyemo, "Energy potentials of organic wastes", Proceedings of the first National Conference on Manufacturing Technology and Engineering in a Development Economy, University of Uyo, Nigeria, 2001, pp. 56 – 61.
- [2] F.D Maramba, "Biogas and Waste Recycling. The Philippines Experience", Academic Press, 1978, pp. 172-202
- [3] I.O Ogunleye and O, Awogbemi, "Determination of thermo-physical properties of eight varieties of sawdust". Journal of Research in Engineering, Vol. 4 No. 4, 2007, pp 8 - 14.
- [4] I.O Ogunleye and O, Awogbemi, "Effects of silica clay on thermo-physical properties of iroko sawdust cement board", International Journal of Science and Technology, Vol. 2 No. 7, 2012, pp 479 – 485
- [5] E.J Da –Silva, "Biogas Generation Developments, Problems and Tasks Overview" Division of Scientific Research and Higher Education UNESCO, Paris, France, 1979, pp. 1 – 19.
- [6] J.P Bolte, D.T Hill and T.H Wood, "Anaerobic Digestion of Screened Waste Liquids in Suspend Particles Attached Growth Reactors", Trans. of the ASAE, Vol. 29, No 2, 1986, pp 543–549.
- [7] O.P Chawla, "Advances in Biogas Technology" India Council of Agricultural Research New Delhi, 1986, pp. 144
- [8] A. M Mshandete and W. Parawira, "Biogas technology research in selected sub-saharan African countries- a review", African Journal of Biotechnology, Vol. 8 (2), 2009, pp116-125.
- [9] L.L Anderson and D.A Tillman, "Fuels from wastes" Academic press, 1977, pp 2 – 12
- [10] S.B Adeyemo and A.A Adeyanju, "Improving Biogas Yield Using Media Materials", Nigerian Journal of Mechanical Engineering, Vol. 2(1), 2004, pp. 14 – 21.
- [11] I.N Itodo, E.B Lucas, and E.I Kucha, "The Effects of Feed Composition on Digester Performance", Applied Science publisher Ltd. London, 1992, pp. 913 – 930.